TKK Dissertations 12
Espoo 2005

CONTROLLING IRON AND COPPER PRECIPITATION IN SILICON WAFERS

Doctoral Dissertation

Hele Savin

Helsinki University of Technology
Department of Electrical and Communications Engineering
Electron Physics Laboratory

TKK Dissertations 12
Espoo 2005

CONTROLLING IRON AND COPPER PRECIPITATION IN SILICON WAFERS

Doctoral Dissertation

Hele Savin

Dissertation for the degree of Doctor of Science in Technology to be presented with due permission of the Department of Electrical and Communications Engineering for public examination and debate in Large Seminar Hall of Micronova at Helsinki University of Technology (Espoo, Finland) on the 21st of October, 2005, at 12 noon.

Helsinki University of Technology
Department of Electrical and Communications Engineering
Electron Physics Laboratory

Teknillinen korkeakoulu
Sähkö- ja tietoliikennetekniikan osasto
Elektronifysiikan laboratorio

Distribution:
Helsinki University of Technology
Department of Electrical and Communications Engineering
Electron Physics Laboratory
P.O. Box 3500
FI - 02015 TKK
FINLAND
Tel. +358-9-451 2322
Fax +358-9-451 5008
URL: http://www.tkk.fi/Units/Electron/
E-mail: hele.savin@tkk.fi

ISBN 951-22-7872-3
ISBN 951-22-7873-1 (PDF)
ISSN 1795-2239
ISSN 1795-4584 (PDF)
URL: http://lib.tkk.fi/Diss/2005/isbn9512278731/

TKK-DISS-2047

Otamedia Oy
Espoo 2005

HELSINKI UNIVERSITY OF TECHNOLOGY
P.O. BOX 1000, FI-02015 TKK
http://www.tkk.fi

ABSTRACT OF DOCTORAL DISSERTATION

Author Hele Savin

Name of the dissertation

Controlling iron and copper precipitation in silicon wafers

Date of manuscript 20.9.2005 | Date of the dissertation 21.10.2005

☐ Monograph ☑ Article dissertation (summary + original articles)

Department Electrical and Communications Engineering
Laboratory Electron Physics
Field of research Semiconductor technology
Opponent(s) Prof. Dieter K. Schroder
Supervisor Prof. Juha Sinkkonen
(Instructor)

Abstract

This thesis studies the two most common transition metals in silicon - copper and iron. The purpose of the experiments and theoretical calculations presented in this thesis is to increase the current knowledge of the precipitation behavior of these metals under different processing conditions. The study also includes the development of recombination lifetime methods for impurity characterization in silicon.

A method to measure trace copper contamination in silicon using the microwave photoconductivity decay is proposed. The method is based on the observation that copper precipitates can be created using light activation. It is shown that external charge on wafer surfaces can reduce the copper out-diffusion, which extends the applicability of the method. Moreover, oxide precipitates are found to increase the sensitivity of the method.

An analytical solution to the current continuity equation for excess carriers in an epitaxial structure under time dependent optical excitation is derived. In addition, some analytical approximations are developed and numerical calculations are made to check their accuracy. The built-in potential between the epitaxial layer and the substrate is taken into account and also the light induced barrier lowering is included in the model. The barrier lowering is found to be noticeable and can affect the effective lifetime by up to two orders of magnitude.

Several annealing profiles and contamination levels are used to study the iron gettering behavior at varying supersaturation levels. It was found that the gettering efficiency depends strongly on the initial iron concentration and considerably high supersaturation is needed to initiate the gettering. The results are discussed from the perspective of thermodynamics.

The thermal stability of internally gettered iron is studied experimentally by deep level transient spectroscopy. The experiments reveal that the dissolution is a reaction limited process. The simulations of iron re-dissolution show that instead of simulating only the final cooling, it is important to simulate the whole thermal cycle. This is important since low thermal budgets are becoming more and more common in the IC technology.

Keywords photoconductivity decay, recombination lifetime, epitaxial, internal gettering, oxide precipitates

ISBN (printed) 951-22-7872-3 | ISSN (printed) 1795-2239
ISBN (pdf) 951-22-7873-1 | ISSN (pdf) 1795-4584
ISBN (others) | Number of pages 34 + app. 39

Publisher Helsinki University of Technology, Electron Physics Laboratory

Print distribution Helsinki University of Technology, Electron Physics Laboratory

☑ The dissertation can be read at http://lib.tkk.fi/Diss/ 2005/isbn9512278731/

Preface

This dissertation is the result of a fruitful collaboration between Lawrence Berkeley National Laboratory (LBNL) and Helsinki University of Technology (HUT). The dissertation is part of several research projects at HUT that I have been involved in (*Characterization of defects in novel silicon based material systems, Oxygen precipitation in silicon and its technical applications, Microscopic defect dynamics in silicon*). The projects have been funded by the Academy of Finland, Finnish National Technology Agency, Okmetic Oyj, MAS Oy and VTI Technologies Oy. Financial support from the Graduate School in Electronics, Telecommunications and Automation (GETA) and private organizations (Heikki and Hilma Honkanen, Jenny and Antti Wihuri, Walter Ahlström and Finnish Technology foundations) are also acknowledged.

I gratefully acknowledge all those who have provided help and encouragement during the writing of this thesis. First of all, I wish to express my gratitude to Professor Juha Sinkkonen, the head of the Electron Physics Laboratory, for providing me the opportunity to do this work, and for his advice as the supervisor of my dissertation. I feel honored to have Professor Dieter Schroder from Arizona State University as my opponent at the defence of the dissertation. I am also grateful for the pre-examiners Dr. Simo Eränen and Dr. Atte Haapalinna, who have both provided me with valuable comments and suggestions for improvements.

I am very grateful to my colleagues at Electron Physics Laboratory for their pleasant co-operation. Especially, I want to thank Antti Haarahiltunen, Marko Yli-Koski and Olli Anttila for fruitful discussions and exchange of ideas. Thanks are also due to Eero Saarnilehto for making some of the copper measurements and Charlotta Tuovinen for revising my English.

I am thankful for Professor Eicke Weber at UC Berkeley for the pleasant and fruitful year I had in Berkeley. I enjoyed enormously working together with the top scientists in this field, *i.e*., the silicon team members Dr. Andrei Istratov, Peng Zhang, Tonio Buonassisi and Ravinder Sachdeva. I am further indebt to Dr. Tamara Radetic, Dr. Chengyiong Song and Dr. Alberto Tolley for assisting me with the TEM analyses at the National Center for Electron Microscopy (NCEM) at Berkeley. I also wish to express warm thanks to the director of Semilab Inc., Dr. Tibor Pavelka, for the opportunity to perform TID and SIRM measurements with their equipment.

Finally, I want to thank my parents for their support and encouragement throughout my studies. My special thanks go to my husband Mikko for reminding me of what is truly important in life.

Espoo, September 2005

Hele Savin

Contents

List of publications

This thesis consists of an overview and the following selection of the author's publications:

I. H. Väinölä, M. Yli-Koski, A. Haarahiltunen, and J. Sinkkonen, *Sensitive copper detection in p-type CZ-silicon using μ-PCD*, Journal of the Electrochemical Society, Vol. 150, G790-G794 (2003).

II. H. Väinölä, E. Saarnilehto, M. Yli-Koski, A. Haarahiltunen, J. Sinkkonen, G. Berenyi, and T. Pavelka, *Quantitative copper measurement in oxidized p-type silicon wafers using microwave photoconductivity decay*, Applied Physics Letters, Vol. 87, 032109 (2005) .

III. H. Väinölä, J. Storgårds, M. Yli-Koski, and J. Sinkkonen, *Evaluation of effective carrier lifetime in epitaxial silicon layers*, Solid State Phenomena, Vols. 82-84, 771-776 (2002).

IV. H. Väinölä, J. Storgårds, M. Yli-Koski, and J. Sinkkonen, *Light induced change on the built-in potential of p/p+ structures and its effect on carrier lifetime measurements*, Materials Science and Engineering, Vols. B91-92, 421-424 (2002).

V. H. Väinölä, A. Haarahiltunen, E. Saarnilehto, M. Yli-Koski, J. Sinkkonen, and O. Anttila, *Enhancement of internal gettering efficiency of iron by low temperature nucleation*, The Electrochemical Society Proceedings Vol. 05, High Purity Silicon VIII, Editors: C.L. Claeys, M. Watanabe, R. Falster, P. Stallhofer, p.160-164 (2004).

VI. P. Zhang, H. Väinölä, A. Istratov, and E. R. Weber, *Thermal stability of internal gettering of iron in silicon and its impact on optimization of gettering*, Applied Physics Letters, Vol. 83**,** 4324-4326 (2003).

VII. H. Väinölä, P. Zhang, A. Haarahiltunen, A. Istratov, and E. R. Weber*, Simulations of iron re-dissolution from oxygen precipitates in CZ-silicon and its impact on gettering efficiency*, Solid State Phenomena, Vols. 95-96, 581-586 (2004).

In the overview these publications are referred to by their roman numerals.

Author's contribution

The author Hele Savin (née Väinölä) has had an active role in all stages of the research reported in this thesis. She has written the manuscripts for Publications I-V, VII and actively participated in writing Publication VI. In Publications I and II she planned the experiments jointly with the co-authors, contributed to the preparation of the samples, participated in the μ–PCD and TID measurements and interpreted the results. She is responsible for the theoretical formulation and simulations of Publications III and IV. She prepared the samples and carried out the TEM analysis presented in Chapter 2. The sample preparation and lifetime measurements in Publication V were carried out by the author. The results were interpreted together with the co-authors. The author is responsible for the formulation and implementation of the simulations in Publications VI and VII.

In addition, the author has presented the results of the work at major international conferences including the 9th International Conference on Defects – Recognition, Imaging and Physics in Semiconductors (DRIP) in Rimini (Italy) in 2001, Gettering and Defect Engineering in Semiconductor Technology (GADEST) in S. Tecla (Italy) 2001, and the Electrochemical Society Meetings in Salt Lake City (USA) 2002 and Honolulu (USA) 2004.

1 Introduction

This year we are celebrating the 40th anniversary of the famous Moore's Law.[1] Gordon Moore's prediction that the number of transistors on integrated circuits, and hence the computing power, would double every 12 to 18 months has been maintained over the years and continues unabated today. This has been possible through the continuous improvements and developments in silicon wafer technology and device manufacturing: the semiconductor industry is nowadays able to manufacture devices even at a nanometer scale.[2] To ensure the efficiency of these extremely complex and miniaturized components, requirements for material purity and structural perfection have become very stringent. Even small quantities of foreign atoms or crystal defects in silicon wafers can be detrimental to device performances and can dramatically degrade long-term stability of final products resulting in yield losses.

Transition metal contaminants, such as iron and copper, are considered especially harmful defects as they, among other things, *i*) introduce deep levels in the bandgap degrading the carrier lifetime, *ii*) precipitate easily at the Si/SiO_2 interface degrading the gate oxide integrity in MOS devices, *iii*) have high diffusivity, which can result in fast contamination of large wafer areas even from point sources, *iv*) have a strong temperature dependency of the solubility, which facilitates formation of metal precipitates and/or complexes as the metals supersaturate easily during cooling.[3]

The low levels of acceptable metal contamination require utmost purity during all steps of the material and device manufacturing processes. However, it can be difficult or even impossible to eliminate all contamination on a production line at a reasonable cost. Fortunately, it is not necessary to have entirely defect-free wafers as the components use only the near-surface region of the wafer. In integrated circuit (IC) applications, the major part of the wafer bulk acts only as a substrate for components and the defects there do not affect the device performance. Thus, instead of pursuing towards defect-free silicon wafers, it is easier to concentrate on driving contaminants away from the component area and redistributing them in predetermined regions, where their presence is not harmful. This process is called gettering. When impurity gettering is under control, it does not only enhance the performance of devices under normal process conditions, but it can also salvage the wafers in case of accidental contamination.

Gettering processes can be divided into two categories called either Internal Gettering (IG) or External Gettering (EG). In IG the sinks for contaminants include oxide precipitates and related defects in the bulk while in EG the gettering sites are usually formed in the back surface of the wafer, for instance, through mechanical damage. With device shrinkage IG has gradually started to replace EG.[4] IG is a very attractive method for impurity control and it has been studied extensively over the years. So far, however, a full understanding of the gettering mechanism has not been achieved. A better knowledge of the behavior of transition metals and defect dynamics in silicon is essential in controlling the impurities by gettering. Only with increased understanding it is possible to create fully predictive models for transition metal behavior under different processing conditions, and eventually, optimize the device yield.

The low acceptable impurity density also raises a challenge in metrology as the defect densities are close to the limit of the present capabilities of most characterization tools. The situation is even more challenging in thin layers: denuded zones in IG wafers and epitaxial silicon layers. There is a constant need for sensitive and reliable in-line detection tools in the production environment to identify and diagnose issues before they destroy the yield.

Contactless recombination lifetime methods represent a good example of in-line monitoring of transition metal contamination as measurements are fast, non-destructive, and sensitive to the measured defect concentrations. However, recombination lifetime methods cannot be used as such to identify different contaminants as the measured lifetime is always an effective value describing the general quality of the sample, where different recombination events take place simultaneously. For impurity identification, a unique fingerprint of the contaminant is needed. Iron can be identified by a well-known flashlight dissociation of iron-boron pairs, which results in a decrease in the recombination activity with a characteristic time constant.[5,6] Identification of copper by lifetime methods, on the other hand, has been considered impossible so far.

The above challenges in metrology are approached in this thesis by developing the recombination lifetime method, extending its applicability. First, the focus is placed on the discovery of identifying and measuring copper using the recombination lifetime method (Publications I and II). Secondly, we study the recombination lifetime measurements in epitaxial silicon wafers, mainly on a theoretical level (Publications III and IV). As regards to gettering, we study the gettering efficiency under a variety of processing conditions obtaining further knowledge and understanding of the gettering mechanism (Publication V). Finally, the thermal stability of gettering sites and its impact on process optimization is investigated (Publications VI and VII).

2 Development of recombination lifetime methods

Minority carrier recombination lifetime is an excellent parameter for characterizing the purity of today's high quality materials as it is easy to measure, commercial equipment are available and it can be used to detect low defect concentrations.[7,8,9] Moreover, the recombination lifetime measurements are fast and nondestructive allowing in-line monitoring, which makes them suitable also for the industrial environment. For these reasons the IC-industry is using lifetime measurements widely to monitor the cleanliness of their processes. The most common methods to measure recombination lifetime (or minority carrier diffusion length) include photoconductivity decay (PCD), surface photovoltage (SPV) and electrolytic metal analysis (Elymat). The main principles of these methods are well covered in Ref. 10 (PCD and SPV) and in Ref. 11 (Elymat).

2.1 Sensitive copper detection in *p*-Si

The identification and measurement of different contaminants from lifetime measurements is a challenging task. So far only iron can be measured on a quantitative level using the well known method developed by Zoth and Bergholz.[12] The method is based on the dissociation of iron-boron (Fe-B) pairs using thermal or optical activation. Interstitial iron, Fe_i, has a different recombination activity as compared to Fe-B, and the dissociation/association of Fe-B pairs have a characteristic time constant that depends on the boron concentration.[13] These characteristics allow identification and quantitative measurement of iron using recombination lifetime methods.

Publications I and II explore the possibility of using recombination lifetime for the identification and measurement of copper in silicon. The publications address the following problems. Firstly, we knew that interstitial copper tends to outdiffuse to the wafer surfaces in *p*-Si and therefore copper detection in the bulk was considered impossible. We found a solution to this problem in a positive corona charge, which was deposited on the oxidized wafer surfaces. As interstitial copper is positively charged, the Coulombic repulsion prevents copper from outdiffusing and the copper can be kept in the bulk in the interstitial form for long periods of time, in fact, even years. Moreover, we have shown that by using corona charge of opposite polarities, it is possible to shift copper back and forth between the surface and the bulk.[14]

The second problem concerned the fact that copper does not have an effect on the recombination lifetime in p-type silicon when it is present in the interstitial form.[15] We knew though, that copper precipitates are extremely efficient minority carrier recombination sites.[16,17] In Refs. 16 and 17 it was concluded that copper precipitates in p-Si only when the copper concentration is high: interstitial copper acts as a donor in p-type silicon and the subsequent Fermi-level increase changes the charge state of the copper precipitates to negative or neutral. Thus, the electrostatic precipitation barrier between interstitial copper ions and precipitates disappears or even changes to attraction. We found out that, similarly, increasing the electron quasi-Fermi level using high-intensity light, enables copper to precipitate even at low concentrations at room temperature. We show in Publication I that the

onset of precipitation takes place at the same Fermi-level position as in Ref. 16. In short, the use of high intensity light is the solution to the detection of copper by a lifetime method.

Thirdly, we needed to improve the detection limit of the method. A hint for this was found from Ref. 18, in which small oxygen clusters were found to have a major effect on the copper precipitation as compared to as-grown wafers. We noticed in our experiments that small oxide precipitates can indeed be used to improve the detection limit and thus lower copper concentrations can be measured.

To confirm that copper stays in the bulk also during illumination, we used Silvaco ATLAS Device Simulation[19] and PC1D Simulation[20] software to simulate the surface band-bending. According to our simulations, the band-bending is in the order of 0.2 eV during illumination when using a positive corona charge of 1 $\mu C/cm^2$ on the wafer surfaces. Shabani *et al.* reported that 0.2 eV band bending gives the outdiffusion time constant of one day at 20ºC.[21] Therefore, we can expect that in our experiments copper outdiffusion is insignificant during illumination. M. Boehringer *et al.* have, however, found opposite results quite recently.[22] They propose that the illumination causes the collapse of the electrostatic barrier in the near-surface region, and outdiffusion of copper occurs simultaneously with precipitation. This was demonstrated by measuring the interface trap density as a function of illumination time. Whether outdiffusion or precipitation prevails depends on the experimental conditions. They deposited copper on the bare silicon wafer, not through an oxide layer, which can result in different surface conditions and may explain the different result. It is worth mentioning that copper outdiffusion and precipitation are two different processes, each having their own electrostatic barrier. Therefore, the reduction of the electrostatic barrier for copper precipitation due to illumination does not conflict with the residual outdiffusion barrier.

A combination of these findings resulted in a method for the measurement of copper in p-type silicon using microwave photoconductivity decay (μ-PCD). As a summary, the procedure to measure copper using light activation is as follows. The wafers to be measured must be p-type and oxidized, the minimum oxide thickness being 5 nm. After suspected contamination, a positive corona charge of about $1\mu C/cm^2$ is deposited on both wafer surfaces. After deposition of the corona charge, the contamination can be measured at any time as it does not change with time. Before light illumination an initial lifetime of the wafer is measured conventionally with μ-PCD. The wafer is then exposed to light, either spot like or large area illumination, depending on the needs to perform mapping or just a single point measurement. For low-level contamination, a high intensity spot-like illumination source is preferred. The illumination time needed to complete the reaction depends on the copper contamination level, the density of oxide precipitates and the activation light intensity; basically it can vary between 10 min to several hours. After light illumination, the wafer is measured again conventionally with μ-PCD. If the wafer has copper contamination, the lifetime decreases from its initial value. From the difference between the initial lifetime value and the value after light illumination, one can evaluate the copper concentration using Equation 2 in Publication II.

Ramappa and Henley reported a similar method in 1999, which was based on SPV.[23,24,25] At that time they believed that the observed lifetime decrease was due to extended substitutional defects in silicon. We believe that they observed in their experiments the same phenomenon

as we did, *i.e.*, copper precipitation. The main difference in their work as compared to ours is that they used SPV and thus a low injection measurement. At a low injection measurement, it is difficult to separate copper from iron contamination as both contaminants decrease the recombination lifetime after illumination. In addition, they did not use corona charge nor oxide precipitates so the measurement needed to be carried out immediately and some of the copper might escape the measurement because of partial outdiffusion. The bulk copper concentration was not calibrated and no estimate for the detection limit was given.

The main advantage of our method is that the measurement does not need to be carried out immediately. Another major advantage is that even though the method is based on the lifetime difference before and after optical activation similar to iron detection, it cannot be confused with iron. First of all, the lifetime changes in the opposite direction after light activation. Secondly, the time constant is in a completely different time range. Due to the different time constant, it is possible to detect both iron and copper with a single measurement from the same point. Thirdly, the copper induced lifetime change is permanent (Publication I) and the formed defects are thermally very stable.[26] It is well-known that after dissociation of Fe-B pairs, iron and boron start forming pairs again at room temperature within hours. Thus, the reaction is reversible.

This method has also the potential to reveal any inhomogeneous copper contamination through lifetime mapping similar to iron. This is demonstrated in Figure 1. A spot-like iron contamination was deposited on the back surface of an as-grown p-type silicon wafer with a resistivity of 10-20 Ωcm. Subsequent iron indiffusion was performed at 900ºC for 30 minutes in an oxidizing ambient. Copper was then deposited next to the iron contamination spot, *i.e.*, on the oxidized surface. This procedure prevents unintentional iron contamination at the intentional copper contamination area. Fig. 1 (a) shows a conventionally measured lifetime map of an iron and copper contaminated wafer. Fig. 1 (b) shows the lifetime map of the same wafer after light illumination. The light illumination took 10 minutes with a light power of 0.2 W/cm^2. This was found to be enough to complete the copper reaction. The copper concentration can be measured on a quantitative level from the lifetime maps using the data given in the Publication II. Iron and copper concentrations were calculated to be in the order of 10^{12} cm^{-3} and 10^{13} cm^{-3}, respectively.

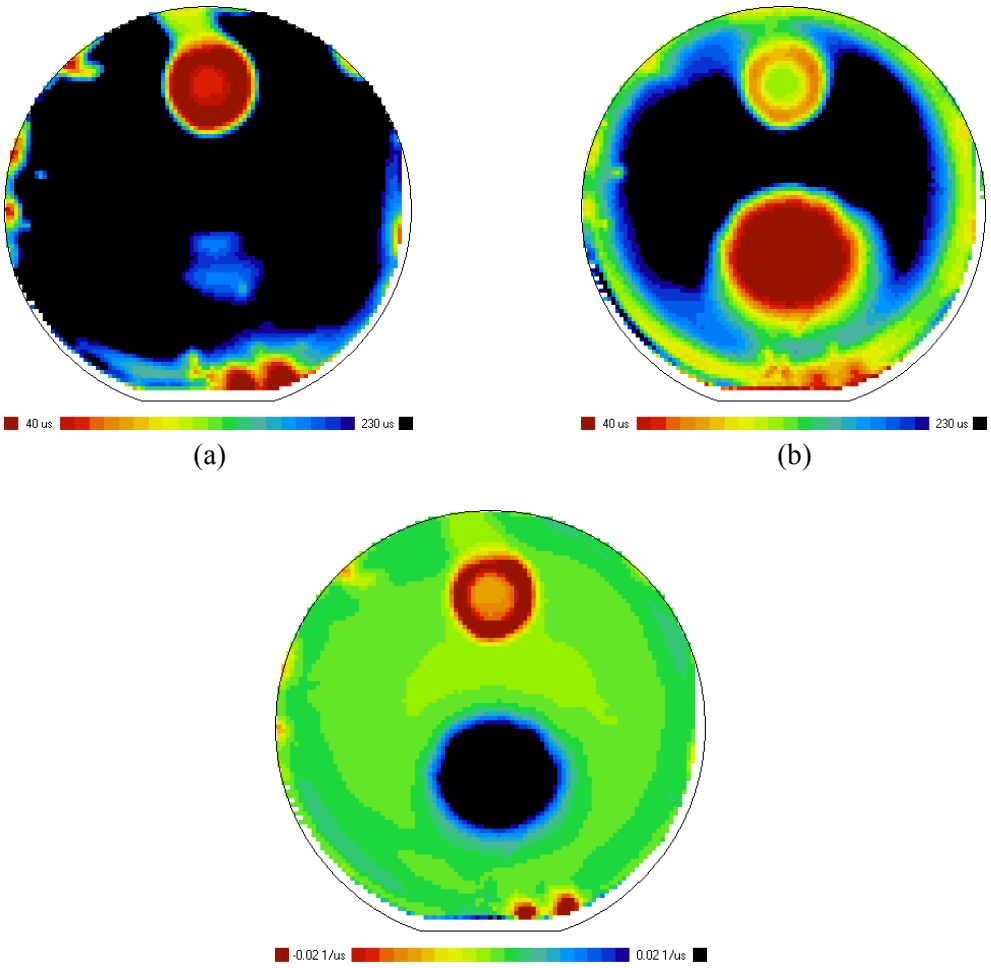

Figure 1. a) A conventionally measured lifetime map with spot-like iron and copper contaminations. The iron contamination is clearly visible in the upper part of the wafer (lifetime is about 25 µs) while the lifetime in the copper contaminated area is above 200 µs. b) A lifetime map of the same wafer after 10 minutes of light illumination (0.2 W/cm^2). The lifetime has increased in the Fe contamination area to about 100 µs while the lifetime has decreased in the copper contamination area to about 20 µs. c) Subtracted lifetime map of a) and b).

Figure 1 c) shows the subtracted maps of Fig.1 a) and b), *i.e.*, the inverse of lifetime

$$\frac{1}{\tau} = \frac{1}{\tau_{after}} - \frac{1}{\tau_{before}} \quad , \tag{1}$$

where τ_{after} is the lifetime map of Fig. 1(b) and τ_{before} is the lifetime map of Fig. 1(a). The red spot reveals the Fe contamination (negative value) and the blue spot reveals the copper contamination (positive value). The green area represents the area where the lifetime does not change due to light illumination therefore representing the uncontaminated area.

We have recently performed bulk micro-defect (BMD) density measurements on the copper contaminated samples using the Scanning Infrared Microscopy (SIRM) by Semilab Inc. The

results reveal that the light activated copper defects are detectable by SIRM. Figure 2 (a) shows a lifetime map of the copper contaminated sample ([Cu] ~ 8×10^{13} cm^{-3}, no oxide precipitates) after light illumination, which was performed about 45 mm from the left edge of the sample. Figure 2 (b) shows the SIRM line scan result of the same sample. It can be seen that near the area of the light illumination, the defect density increases compared to the non-illuminated area. The defect density of 3×10^{7} cm^{-3} in the illuminated area can be considered to be the lower limit of the defect density, due to a bad surface preparation.

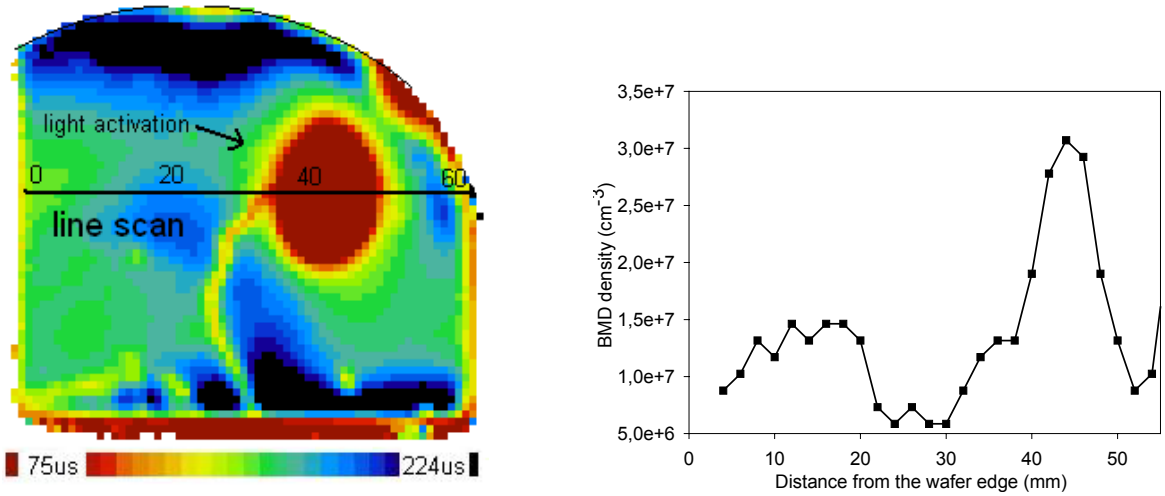

a) b)

Figure 2. a) Lifetime map of copper contaminated sample. The light illuminated spot is clearly visible. The centre of the illumination spot is located about 45mm from the left sample edge. b) Line scan of the same wafer by SIRM.

These SIRM results show promise for studying the quantitative density and size of the copper precipitates formed during light illumination. To obtain more accurate information, SIRM measurements on samples that have varying copper concentrations and oxide precipitate densities are recommended.

2.2 Characterization of layered structures

Recombination lifetime methods are effective tools for the characterization of silicon bulk material, as shown in the preceding subchapter. However, the situation is much more complicated when monitoring the quality of the thin semiconductor layer present in, for instance, epitaxial or IG wafers: intrinsic recombination properties of the thin layer are easily masked by the recombination at the surface and in the substrate. Publications III and IV discuss the possibilities to use recombination lifetime measurements in epitaxial silicon wafers on a theoretical level. The main results are summarized here and comparison to literature is also given.

2.2.1 Epitaxial wafers

Silicon epitaxy is used to improve the performance of bipolar and some CMOS devices. Epitaxy also allows better control of doping profiles and layer thicknesses compared to, for instance, ion implantation. Several groups have studied the applicability of lifetime methods for the characterization of thin epitaxial layers (epi). There are also a few commercial characterization tools for epitaxial layers: improved μ-PCD by Semilab Inc.[31] and Epi-Tau FAast 330 system by Semiconductor Diagnostics,[9] the latter being a frequency-dependent ac SPV. Both methods have improved sensitivity to measure epitaxial layers although in both methods the measured lifetime is still strongly influenced by surface recombination. The most recent papers by Park et al.[27] and Schroder et al.[28] present a comprehensive review of the experimental work on this topic. This chapter summarizes the theoretical formulations of the papers on the same topic.

In Publications III and IV we make a careful theoretical analysis of the lifetime measurement in a two-layer structure. In order to be able to extract the recombination parameters, we focus on the physical principles of the measurement rather than practical details, with the main emphasis on the correct interpretation of the measurement results. The current continuity equation for excess carriers is solved analytically in an epitaxial structure under time dependent optical excitation. Built-in potential is taken into account, which affects the carrier diffusion from epi to substrate or vice versa. In addition, some analytical approximations are developed and numerical calculations are made to check their accuracy. The results show that the extraction of recombination parameters of epi layers is simplest in a *p/p* or *n/n* structure and a bit more demanding in p/p^+ or n/n^+ but possible by means of the models presented in Publication III.

An accurate solution for the bulk lifetime of the epilayer, τ_1, is obtained from the following equations. The measured effective lifetime is

$$\frac{1}{\tau_{eff}} = \lambda \ , \quad \gamma_j^{\,2} = \frac{1}{D_j}\left(\lambda - \frac{1}{\tau_j}\right) \ , \ j=1,2 \tag{2}$$

where subscript 1 refers to the epilayer and 2 to the substrate. D_j is the diffusion coefficient for minority carriers and τ_j the bulk recombination lifetime. The epilayer lifetime can be calculated by substituting Eq. 2 into the following equation and finding the first root of λ (or τ_1)

$$\tan(\gamma_2(w-d)-\theta_2)\tan(\gamma_1 d \ +\theta_1) = \frac{D_1\gamma_1}{D_2\gamma_2}e^{q\phi/kT} \ , \tag{3}$$

$$\tan\theta_1 = \frac{\gamma_1 D_1}{s_1}, \ \tan\theta_2 = \frac{s_2}{\gamma_2 D_2} .$$

Here s_1 and s_2 are the surface recombination velocities at the front and back surfaces, respectively, w is the wafer thickness, and d is the epilayer thickness. A simpler approximation to extract the epilayer lifetime is presented in Publication III.

Epitaxial structures with a similar (and rather low) doping density both in the epi and the substrate (*p/p* or *n/n*) cause no sensitivity problem in detecting the photoconductivity signal as compared to low resistivity samples. Another advantage is that in these structures there is no built-in potential barrier at the interface, which makes the theory much simpler. On the other hand, charge carriers are not confined to epi but can freely diffuse to the substrate, which

means that the measured lifetime is always an effective value and is strongly influenced by the recombination in the substrate. H. Takashi and T. Maekawa[29] formulated a solution to the steady state continuity equation in this case and found as a simple approximation as the layer thickness averaged lifetime

$$\frac{1}{\tau_{eff}} = \frac{1}{\tau_{epi}}\frac{d}{w} + \frac{1}{\tau_{sub}}\frac{w-d}{w} + \frac{2s}{w}. \tag{4}$$

T. Hara et al.[30] used an even simpler approach by assuming the effective lifetime to be equal to the reciprocal sum of the bulk lifetime in epi and substrate $\tau_{eff}^{-1} = \tau_{epi}^{-1} + \tau_{sub}^{-1}$. In their study the surface recombination was omitted. Figure 3 shows a comparison of these models. As expected, the approximate expressions of Publication III and Ref. 29 are almost in agreement with the exact solution. A small discrepancy appears when the epilayer lifetime is small compared to the substrate lifetime. In these cases the approximations tend to underestimate the measured lifetime.

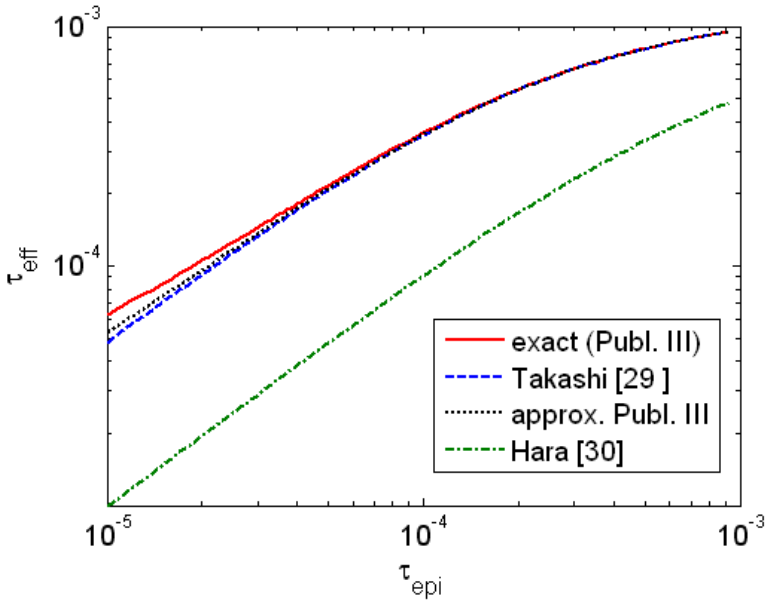

Figure 3. Comparison of different models for epitaxial wafers reported in literature. The simulations were made with the following parameters: epi thickness 50 μm, boron doping 10^{15} cm^{-3} both in the epi and the substrate, bulk lifetime 1 ms and surface recombination velocity 1cm/s on both surfaces.

In the most common epi-structures the epitaxial layer is lightly doped as compared to the substrate (p/p^+ or n/n^+). In this case the built-in potential restricts the diffusion of minority carriers to the substrate although the effective interface recombination cannot be neglected entirely. The interface recombination is stronger the heavier the doping in the substrate is due to the band-gap narrowing. In photoconductivity decay measurements a problem arises from the heavily doped substrate, which has a high absorption of the microwaves, but this can be overcome with a modification of the antenna design.[31] Ogita[32] assumed that the carriers are confined within the epilayer and used an expression similar to the model that is used in homogeneous wafers.[33] Later on Takashi and Maekawa[34] extended their model to n/n^+

structures and included the built-in potential. They found an expression for the interface recombination similar to what is presented in Publication III.

Epi-structures where the epitaxial layer is highly doped as compared to the substrate (p^+/p or n^+/n) are not suited for lifetime characterization. This is because the potential barrier quickly shifts the minority carriers to the bulk and almost no recombination takes place in the epilayer. On the other hand, these structures have almost no practical applications and therefore there is no need to characterize them. Note that our exact solution, presented in Publications III and IV, can be used in all epitaxial structures (p/p, p/p^+, p^+/p, n/n, n/n^+, n^+/n).

In addition to the effective lifetime, the time dependent charge carrier transient decay can be measured by μ-PCD. A time dependent solution for the excess carrier density, presented in Publication III, can be utilized in the characterization of the epitaxial wafers. From the shape of the transient decay and the transient dependency of the generation wavelength we can immediately see which one, epi or substrate, has a higher lifetime. For instance, by varying the generation wavelength, the effective lifetime, *i.e*., the last time constant of the transient, results in the same value but the transient decay is different. The solution presented in Publication III not only allows the determination of the effective lifetime but also the time dependent photoconductivity decay transient.

Publication IV studies the influence of built-in potential on effective lifetime at different injection levels. Both analytical and numerical solutions are shown. Under typical μ-PCD measurement conditions the barrier lowering is noticeable and can affect the effective lifetime even by up to two orders of magnitude. The validity of injection relation in the epi-substrate junction is given in Ref. 35. From a practical point of view, we can always decrease the front surface recombination by different passivation methods but there are only a few means to decrease the interface recombination velocity. One possibility is to reduce the injection level which increases the potential barrier at the substrate-epi interface. This injection level dependency is examined in more detail in Publication IV. Another way is to, if possible, use very lightly doped epilayers, as the interface recombination velocity decreases as the doping decreases in the epilayer. A dependence of interface recombination velocity on the doping density in the substrate is mainly determined by the bandgap narrowing such that the increase in the doping in the substrate results in the increase in the interface recombination velocity.[35,36]

Generation lifetime methods confine the generation volume to the thin epilayer and are more readily applicable than recombination lifetime methods. Nowadays it is also possible to do these measurements without contacts, using corona charge / Kelvin probe. A further advantage is that the surface recombination is less important. Corona oxide semiconductor (Quantox) allows both generation and recombination lifetime measurements from which one can obtain qualitatively both the substrate and epi lifetime.[37]

It could be worth studying the 3D effects in epitaxial structures, but as we show for homogeneous wafers,[38] these effects have almost no significance in most situations. Therefore, the one dimensional analysis that is presented in Publications III and IV is adequate in most cases.

2.2.2 Denuded zone wafers

The defect free near-surface region of the wafer, present in internal gettering wafers, is called the denuded zone (DZ). The DZ wafers can be treated similar to epitaxial wafers when modeling recombination lifetime. Both of them have a two-layer structure with a different bulk lifetime in each layer. Usually the interface between DZ and bulk is not as step-like as in epitaxial wafers but as a first approximation it is a reasonable assumption. Modeling of excess carrier distribution in DZ wafers corresponds the modeling of *p/p* or *n/n* structures as there are no built-in potential due to doping difference. The width of the denuded zone usually varies from 10 μm to 100μm so it is usually much thicker than the epitaxial layer. In the DZ, as it is free of defects, a typical recombination lifetime value is expected to be hundreds of microseconds. The wafer bulk with a lot of recombination active gettering sites, on the other hand, has a much lower recombination lifetime.

At low injection level (SPV) the recombination efficiency of oxide precipitates is larger than at high injection (μ-PCD).[39] Hwang and Schroder[40] presented as an explanation for this a band bending around the precipitate and the presence of a positive fixed charge due to silicon dangling bonds inducing a depletion region around each precipitate in *p*-Si at low injection. This enlarges the minority carrier capture volume of the oxide precipitate and increases its recombination efficiency. At high injection the band bending can be neglected as the inversion layer near the silicon-precipitate interface compensates the effect of a positive fixed charge.[39] Polignano *et al*. took advantage of the sensitivity of the low injection measurement to detect oxide precipitates and proposed a method to measure the denuded zone thickness using SPV.[41]

Figure 4 demonstrates an example of a μ-PCD simulation in DZ wafers based on the model presented in Publication III. It shows that the measured effective lifetime does not significantly depend on the DZ width unless the DZ width is considerably large (over 100μm). Therefore, μ-PCD is not a suitable method to measure the DZ width. The bulk lifetime has a great influence on the measured effective lifetime. As the bulk lifetime is mainly determined by the oxide precipitates (size and density) in IG wafers, μ-PCD measurements could be used to characterize oxide precipitates.

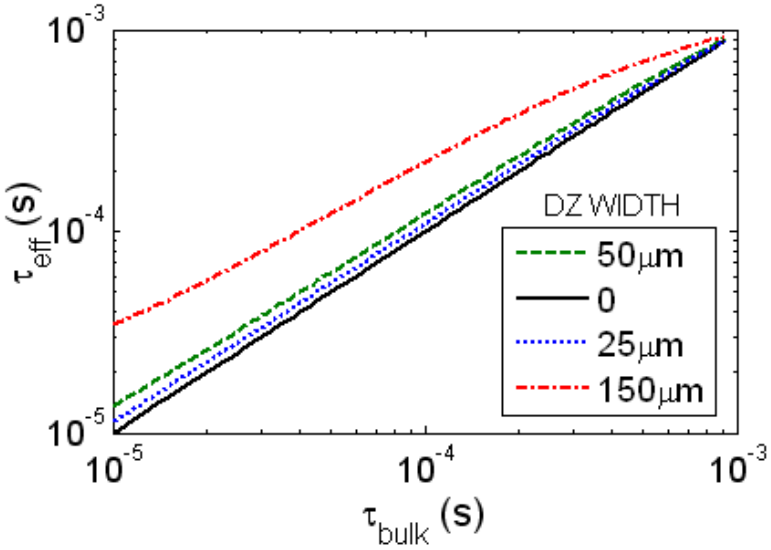

Figure 4. Simulation of effective lifetime in DZ wafers using the model presented in Publication III. The following parameters were used in the simulation: lifetime in the DZ 1 ms, surface recombination velocity 1 cm/s, boron doping 10^{15} cm^{-3}, wafer thickness 500 μm.

Figure 5 shows an example of detecting oxide precipitates experimentally in IG wafers using μ-PCD. The wafers had the conventional High-Low-High anneal (4h or 16h @ 1150ºC + 2 or 4h @ 550ºC or 650ºC + 16h @ 1100ºC) to form the denuded zone and oxide precipitates. The initial oxygen concentration was 14 ppma. The DZ width after anneals was measured to be approximately 40 μm. The oxygen loss was measured by Fourier transform infrared spectroscopy (FTIR) using the ASTM F 121-83 calibration factor. The effective lifetime in the same wafers was measured by μ-PCD. Figure 5 also shows the simulations of the wafers with and without DZ. We can see that the lifetime has some correlation to the oxygen loss, at least at a qualitative level. The simulations show that in this case it is not necessary to take into account the two-layer model.

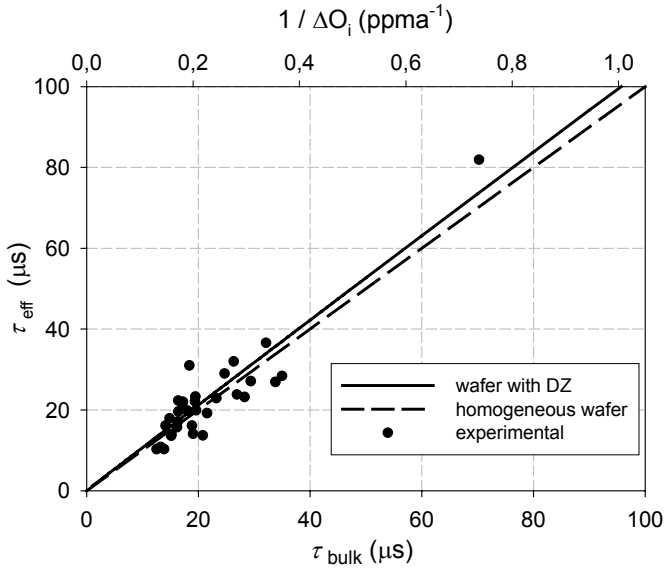

Figure 5. Comparison of experiments and simulations in the case of a denuded zone wafer. The dots represent the experimental data measured by FTIR and μ-PCD. The solid line represents the model presented in Publication III and the dashed line represents the model, which does not take into account the denuded zone. The following simulation parameters were used: wafer thickness 525 μm, lifetime in DZ 500 μs, surface recombination velocity 1 cm/s, boron doping 4×10^{14} cm^{-3}, and DZ width 40 μm.

Figure 6 shows TEM pictures of the oxide precipitates in the samples used in these experiments. A typical diameter of the platelet precipitates was found to be about 100 nm. The density was measured to be in the order of 10^{11} cm^{-3} by defect etching. The density matches the density determined by TEM (Fig. 6 (b)).

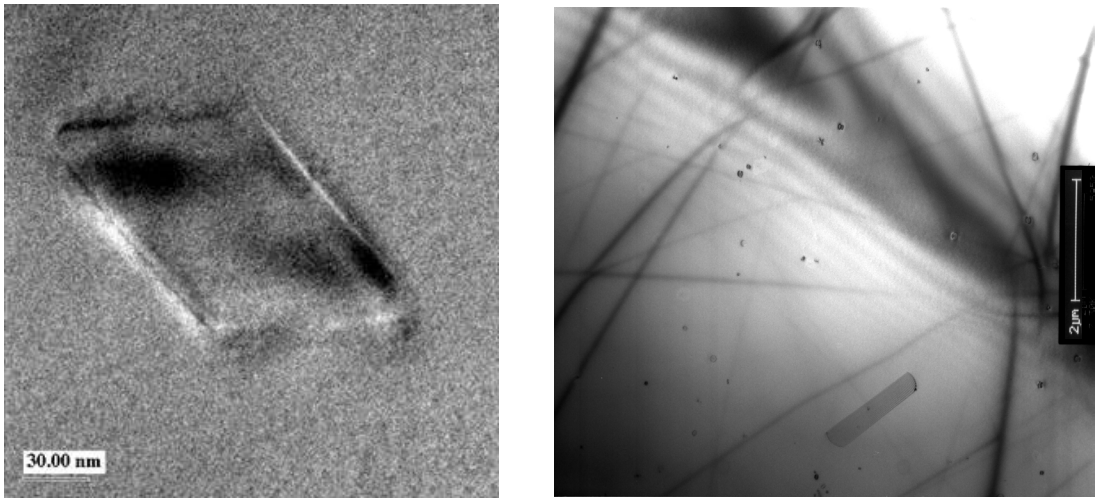

a) b)

Figure 6. TEM pictures of the IG samples. a) A typical size and morphology of the platelet oxide precipitates b) The dark points represent the oxide precipitates with an average distance of 1µm in the 1µm thick sample. This allows the determination of the density of oxide precipitates.

3 Internal gettering of iron

In internal gettering the metal impurities are removed from the active regions of semiconductor wafers and trapped in the bulk by a series of heat treatments. The heat treatments produce oxide precipitates and related crystal defects in the bulk of the wafer acting as gettering sites. Consequently, a high quality defect free zone forms around the active device area. IG has been widely studied since the 1980s, including both experimental and modeling efforts. A comprehensive review of iron gettering can be found in Ref. 42 and 43.

3.1 Effect of supersaturation level on the gettering efficiency

Despite the fact that iron gettering has been studied extensively over the years, a full understanding of the gettering mechanism is still lacking, especially at low supersaturation, *i.e.*, when $C/S \sim 1$, where C is the dissolved iron concentration and S is the solubility of iron in silicon. Most of the papers published on this topic assume that iron precipitation is a diffusion limited process, where each oxide precipitate acts as an effective gettering site.[43,44,45] There are many indications that this may not always be true.

In Publication V we study experimentally the gettering behavior of iron at low supersaturation. The experiments include the measurement of gettering efficiency after a fast cooling with a room temperature step and after traditional slow cooling. Both μ-PCD and Deep Level Transient Spectroscopy (DLTS) are used to measure the gettering efficiency. The use of μ-PCD is justified as we demonstrate in Ref. 46 that both μ-PCD and SPV are capable of measuring the dissolved iron concentration in DZ wafers after calibration with DLTS. The results show that gettering at the initial iron concentration of 10^{13} cm^{-3} does not take place during several hours of anneal at 700ºC. However, with the same initial iron concentration, gettering can be efficient even after 30 minutes of anneal at 700ºC if the wafers go through a low-temperature region before the actual gettering anneal. In the simplest case the low-temperature region can be realized by a fast withdrawal of the wafers from the furnace. The main conclusion drawn from the experiments is that low supersaturation is not adequate to initiate iron nucleation but a low-temperature step is needed, after which the growth of iron precipitates is facilitated.

We made another series of experiments to study further the effect of supersaturation on the gettering efficiency. At this time we changed the supersaturation level by varying the initial iron concentration in addition to the temperature. First, a 15 min homogenization anneal at 1150ºC was performed, which was followed by the Low-High anneals (6h@650°C + 16h@1100°C) to form oxide precipitates. The oxide layer was then removed and intentional iron contamination was carried out at varying indiffusion temperatures: 760ºC, 850ºC or 940ºC with the corresponding solubilities of 1×10^{12} cm^{-3}, 1×10^{13} cm^{-3}, and 1×10^{14} cm^{-3}, respectively. The goal was to get three groups of wafers with different iron concentrations. After indiffusion, both wafer surfaces were carefully cleaned and the wafers were oxidized at 900 ºC for 20 minutes to form an oxide layer of a thickness of about 20 nm. After oxidation the iron concentrations were measured to be 2×10^{12} cm^{-3}, 2×10^{13} cm^{-3}, and 4×10^{13} cm^{-3} in the preceding wafer groups. Before each gettering anneal, the wafers were annealed for 30

minutes at the indiffusion temperature to dissolve the possible iron nuclei that are formed during the ramps after the oxidation anneal. The wafers were then cooled at the rate of 50 ºC/min to the gettering temperature and the actual gettering anneal took 30 minutes at different temperatures (200°C - 800°C). After the gettering anneal, the wafers were cooled to room temperature at the rate of 100 ºC/min. In other words, the outline of the gettering annealing is as follows: 30 min dissolution anneal → cooling 50ºC/min → 30min@200-800ºC → cooling 100ºC/min to RT.

The results of these experiments are shown in Figure 7. At 300ºC the diffusion limits the gettering and almost no gettering takes place at any wafer, which is in accordance with previously published data.[47] Interesting and previously unreported observations can be made at higher temperatures. The dissolved iron concentration depends strongly on the initial iron concentration such that the higher the initial iron concentration the less iron is measured after gettering. It follows that the level of supersaturation plays a significant role in the final gettering efficiency. The effect of supersaturation level is further supported by the observation that a rather high supersaturation is required before precipitation occurs. In all wafers the supersaturation increases the lower the temperature is, thus reducing the measured iron concentration as a function of temperature. In other words, iron must be highly supersaturated and mobile at the same time, which will result in a certain optimum "processing window" where gettering is efficient. The optimum temperature depends on the initial iron concentration and the gettering time. The smaller the initial concentration, the lower the optimum temperature. Notice that the wafer, which has the lowest initial iron concentration, experiences almost no gettering at any temperature. This is because a high enough supersaturation together with high diffusivity is not reached at any temperature.

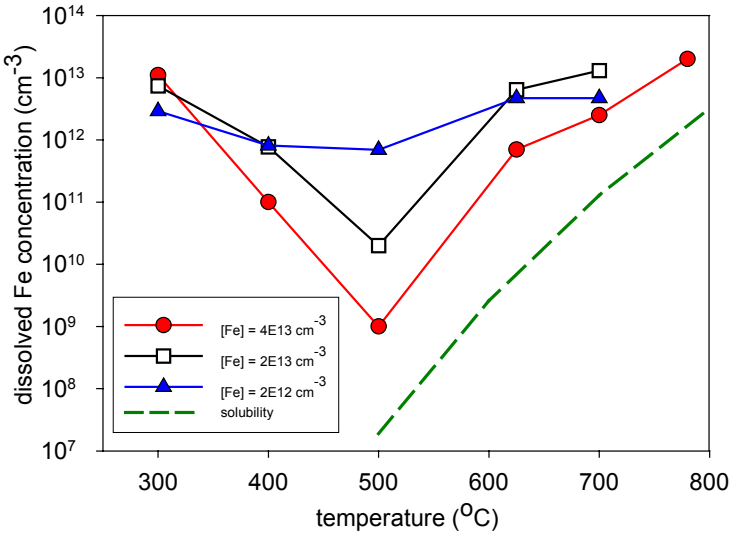

Figure 7. Experimental results of dissolved iron concentration after 30 minutes gettering anneal at different temperatures. Initial iron concentrations are shown in the legend. Also shown is the solid solubility of iron at the corresponding temperatures.

Let us now consider the Ham's diffusion limited precipitation law for fixed radius[48]

$$C(t) = S + (C_0 - S)e^{-t/\tau}, \quad \text{where } \frac{1}{\tau} = 4\pi Dnr \tag{5}$$

where C is the dissolved iron concentration, S is the solid solubility of iron, D is the iron diffusivity, C_0 is the initial dissolved iron concentration, n is the density, and r is the radius of the gettering sites. When modeling IG, the values of oxide precipitate density and radius are often used for n and r. The values for the diffusivity and solubility, needed in the simulations, are quite well known for iron in silicon although some low temperature data is a bit controversial as it is difficult to measure these parameters in the low temperature range. On the other hand, the same material parameters for iron in silicon dioxide have not been known for long. These parameters are essential when simulating, for instance, Silicon On Insulator (SOI) structures. We made some systematic studies on this topic quite recently.[49]

According to Equation 5, precipitation takes place immediately after iron is under supersaturation with a certain time constant τ. Some internal gettering experiments demonstrate that Equation 5, when using the radius and density of oxide precipitates for r and n, is indeed valid for iron.[50,47] However, these experiments were made at very high supersaturation, *i.e.*, the temperature was low enough or the iron contamination level was rather high. In our gettering experiments, made at much lower supersaturation, such an agreement cannot be found. In our samples, the density and the radius of oxide precipitates are in the order of $n = 3\times10^9$ cm^{-3} and $r = 80$ nm according to oxygen precipitation simulations[51],[52] with the given thermal treatment. If we use these values for n and r in Eq. 5, we get a large overestimation both in the gettering efficiency and the width of the processing window. On the other hand, if we take n as the fitting parameter, which depends both on the gettering temperature and the initial contamination level, the experimental results can be modeled by the diffusion limited process (Eq. 5). Alternatively, the process can be considered to be reaction limited, which is discussed in Ref. 43.

The dependence of n on the contamination level and temperature can be explained by the nucleation kinetics, which is well-known from the thermodynamics of phase transformations. The chemical driving force for precipitation from a supersaturated solid solution is given by[15]

$$\mu = kT \ln\left(\frac{C}{S(T)}\right), \tag{6}$$

where C is the dissolved iron concentration and $S(T)$ is the solid solubility of iron. The equation shows that the higher the initial concentration the higher the driving force for precipitation. In addition, a decrease in temperature increases the driving force. The nucleation rate depends strongly on the driving force.[53] It is thus possible that in Fig. 7 the density of nuclei is largest at 300ºC but the diffusion has limited the growth of the precipitates. Eq. 6 also explains the experimental observation that precipitation will not start at the temperature when iron becomes supersaturated, but rather at a lower temperature when the chemical driving force reaches a sufficiently high level to initiate nucleation and growth of precipitates.

Iron solid solubility, *i.e.,* the equilibrium concentration at the interface of a very large iron precipitate, is often used for the value of *S* in Eq. 5. In a rather simple manner, a more realistic precipitation behavior is achieved by replacing the solid solubility of iron by the equilibrium concentration at the interface of the iron precipitate, which depends on the size of the iron nucleus (Gibbs-Thomson equation).[53] It follows that the growth of the heterogeneous precipitation sites that have already gettered some iron are more attractive gettering sites than the ones with no iron. Recently, such simulations were made to explain the experimental results of iron gettering at low supersaturation.[54] However, it is worth to note that the surface energy, the strain and the morphology of the gettering sites as well as the charge state of iron can all have their own contribution to the precipitation. This makes it rather challenging to fully predict the precipitation behavior of iron.

Hieslmair *et al*.[55] have published earlier some interesting experimental data related to this topic. They had iron contaminated wafers with different oxide precipitate densities, which were annealed at gettering temperatures between 200-800ºC. They calculated the number of iron precipitation sites by fitting Eq. 5 to the experimentally measured decay of the dissolved iron concentration. The results are shown in Figure 8. They explained the results as follows: at low supersaturation (high temperature) only a portion of the oxide precipitate surface serves as an iron nucleation site, which reduces the effective number of precipitation sites. Later, Myers *et al*.[43] explained the same observed phenomenon by the reaction limited precipitation. Another explanation for Hieslmair's results could be the above mentioned nucleation kinetics. According to that the number of active gettering sites (oxide precipitates) can be smaller than the real density of the oxide precipitates. In a sample with a high density of possible gettering sites, not all oxide precipitates become active at all temperatures because the dissolved iron is consumed by the growth of stable nuclei and thus the nucleation rate decreases. The sample that has a lower density of possible gettering sites does not "run out" of mobile iron as fast so the effective density matches with the real density of gettering sites. Hieslmair's results are also supported by the observation of Takahashi *et. al*., who demonstrated that large precipitates more easily become active gettering sites. [56]

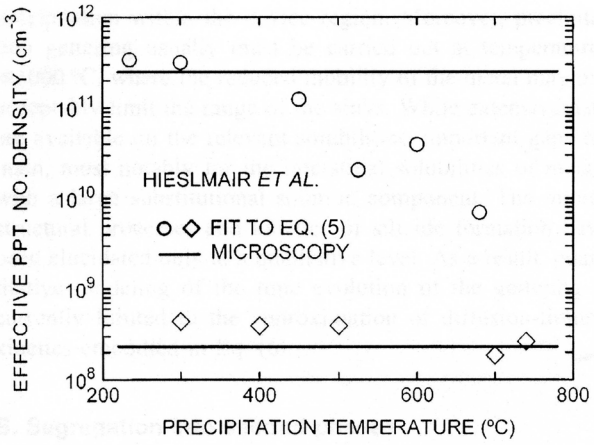

Figure 8. Effective density of gettering sites as derived by fitting Eq. 5 to the experimentally measured decay of the dissolved iron concentration (Ref. 55). The horizontal lines give the actual particle densities obtained from microscopy for the two materials presented.

All these results suggest that the precipitation behavior of iron is very similar to oxygen precipitation. Therefore, we plot the precipitated iron concentration after gettering anneal as a function of initial iron concentration (Figure 9). This figure is often referred as the *s-curve* as it shows the threshold for precipitation. The gettering anneals were the same as in Fig. 7. The curve shifts to the left the lower the annealing temperature is. The curve is very similar to what is usually presented for oxygen in silicon. However, it is good to remember that iron precipitates mostly heterogeneously to existing gettering sites while oxygen can also precipitate homogeneously.

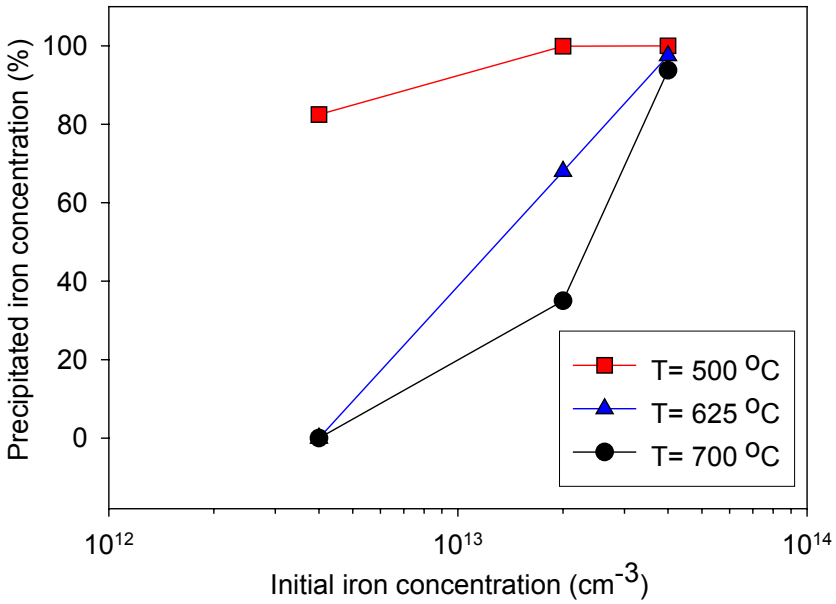

Figure 9. Precipitated iron concentration versus initial iron concentration, *i.e.*, the S-curve. The wafers were annealed for 30 minutes at different temperatures.

The results presented in this chapter and in Publication V lead to the following practical conclusions. Firstly, a high enough supersaturation is required to initiate gettering, similar to oxygen precipitation. Secondly, it seems that internal gettering is effective in case of accidental iron contamination but it is not able to reduce iron contamination in a "clean" process under practical conditions.

3.2 Thermal stability of gettering sites

It is equally important to understand the thermal stability of the gettered impurities as the gettering process itself. In case of copper, several comprehensive studies reveal that copper is not that thermally stable at oxide precipitates when it has precipitated during cooling from a high temperature. As low a temperature as 360ºC has been demonstrated to be enough to dissolve copper back into the silicon matrix.[57] Another study demonstrates a complete dissolution after 1 min at 600ºC.[58]

The dissolution data for iron is much more controversial, which motivated us to make a systematic study on the topic. Publication VI and Ref. 59 study how thermally stable the gettered iron is at oxide precipitates. Based on current knowledge, it was not known if iron, after being gettered by oxide precipitates, *i*) can freely dissolve back to the silicon matrix through diffusion immediately after undersaturation takes place or *ii*) if there is an energy barrier for iron dissolution that is significantly larger than the activation energy for iron diffusion. The former case is referred to as the diffusion barrier and the latter one is referred to as the dissolution barrier. The goal was to obtain experimental data on the dependency of the redissolved iron concentration on annealing time and temperature. The experiments were made with CZ silicon that had an oxide precipitate density of about 5×10^9 cm^{-3} and radius of 88 nm, which were measured by defect etching and TEM. All samples went through the same low-temperature gettering anneal to ensure the samples had the same initial condition. The wafers were then heated at higher temperatures to study the iron dissolution behavior. The dissolved iron concentration was measured by DLTS and a special emphasis was given to measuring also the early stages of the dissolution so that a time dependency of the dissolution process was obtained. Figure 10 shows an example of dissolved iron concentration versus dissolution annealing time at 800ºC and the following fitted curve (solid line)

$$C(t) = C_0\left[1-\exp(-t/\tau_{diss})\right], \qquad (7)$$
$$\tau_{diss}^{-1} = 4.01\times10^4 \exp\left[-(1.47\pm0.10)\,\mathrm{eV}/kT\right] s^{-1},$$

where C_0 and τ_{diss} are the fitting parameters.

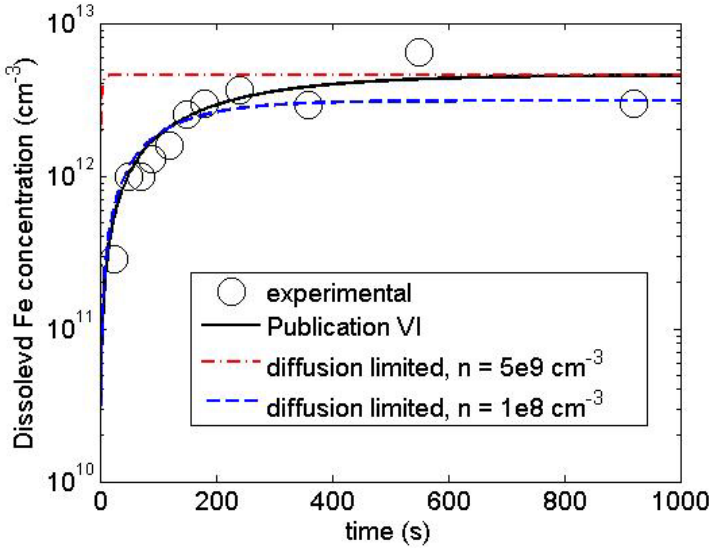

Figure 10. Comparison of experiments and different theories to simulate iron dissolution at 800ºC as a function of annealing time. The circles represent the experimental data, the solid line represent the model in Publication VI, the dashed line represents the diffusion limited model assuming only a limited number of active gettering sites, and the dash-dot line represents the diffusion limited model assuming that each oxide precipitate is an active gettering site.

As discussed previously in the context of gettering, it is possible that not all oxide precipitates are active sinks for iron during gettering. Thus, it is natural that iron dissolves only from the active gettering sites. Figure 10 shows a comparison between the experiments and two different diffusion limited simulations. The first simulation assumes that each oxide precipitate is an active gettering site (dash-dot line) and the second simulation assumes only a limited number of active gettering sites (dashed line). At first look, it seems like the diffusion limited model with $n = 1\times10^{8}$ cm^{-3} active gettering sites matches the experiments well. However, as all samples went through the identical gettering anneal, they must have equal values for n in the beginning of each dissolution anneal independent of the temperature. Now if we compare the obtained activation energy for the dissolution time constant 1.47 eV (from Eq. 7) to the activation energy of diffusion 0.67eV, we can conclude that there seems to be a substantial binding energy between the gettered iron and oxide precipitates.

Using Equation 7 we made simulations of iron re-dissolution during a variety of annealing sequences used in integrated circuit processing. These are reported in Publication VII. The simulations show that a typical rapid thermal annealing does not completely dissolve the gettered iron. Therefore, modeling of gettering in rapid thermal processes (RTP) requires that not only the last cooling but also all preceding heat treatments have to be taken into account. This is important especially when low thermal budgets are becoming more and more common in the IC technology.

Here is a summary of the previously published data on the iron dissolution in silicon and a comparison to our results. Ramappa and Henley made experiments on the thermal stability of iron precipitates in FZ silicon wafers.[60] They did not have oxide at the surface nor any oxide precipitates in the bulk so the iron "precipitation" anneals at low temperature most likely resulted in surface precipitation. Therefore, their results cannot be equated with thermal stability of iron precipitated on oxide precipitates or related defects. McHugo et al.[61] used an iron concentration of about 1×10^{15} cm^{-3} in their experiments and they noticed a complete dissolution after a 10 min anneal at 1050°C, which agrees with our simulation model presented in Publication VI, see Figure 3.(c). On the other hand, they noticed a significant effect of carbon on the thermal stability of iron precipitates. They concluded that carbon reduces the strain field of oxide precipitates and therefore the gettered impurities are not that strongly bound. Aoki and Hara made experiments with both as-grown wafers and IG wafers.[62] They did not find any difference between the wafer types if the dissolution anneal was made at 1000°C. At 750°C and 800°C, on the contrary, the dissolution time constant was approximated to be between 30 and 60 seconds in IG wafers but in as-grown wafers they found a much higher dissolution time constant. Their results for IG wafers are in agreement with our model (Fig. 3 (a) and (b) in Publication VI). Although our experiments were carried out only on one type of IG samples, the model can probably be extended to other IG wafers as well because Aoki and Hara [62] did not find any difference in the iron dissolution behavior in their IG samples and they used wafers with different IG treatments.

4 Conclusions

Today the control of transition metal impurities in silicon plays a crucial role in the semiconductor industry due to the continuous device miniaturization. Even extremely small concentrations of impurities, when present in a harmful form in the device area, can have a detrimental effect on the device yield. Although internal gettering is already a widely used method to control the metal impurities, challenges still remain in fully understanding the interactions between metals and oxide precipitate related defects. In addition, a need to have sensitive and contactless measurement tools for the detection of metal impurities motivates the study of recombination lifetime methods.

This work studied the precipitation behavior of the two most common transition metals in silicon - copper and iron. The experiments were carried out using mostly electrical and optical methods. The impurity concentrations were measured by Deep Level Transient Spectroscopy (DLTS), Transient Ion-Drift (TID), Microwave Photoconductive Decay (μ-PCD) and Total reflection X-ray Fluorescence (TXRF). The density of light-activated copper defects was studied by Scanning Infrared Microscopy (SIRM). Fourier Transform Infrared Spectroscopy (FTIR) was used to measure the precipitated oxygen concentration. In addition, Transmission Electron Microscopy (TEM) analyses were performed to determine the density and size of the oxide precipitates. Some of the experimental studies were complemented with theoretical calculations.

Previously, low copper concentrations in silicon have been considered to be very difficult or even impossible to detect by recombination lifetime methods. This work demonstrates how to measure low copper concentrations using the μ-PCD in combination with light activation. The method is based on the following observations *i*) copper can be kept in the interstitial form in the bulk using a positive corona charge on the wafer surfaces *ii*) copper forms active recombination centers under light illumination *iii*) small oxide precipitates further enhance the recombination activity of light activated copper defects. The method is readily applicable and it allows measurements at a quantitative level. In addition, simultaneous iron measurements and whole wafer mappings are possible, which helps to reveal the sources of contamination. In the future, it would be interesting to study the temperature and injection level dependency of the copper related recombination lifetime. Additional scanning infrared microscopy measurements are also a necessity in achieving a complete understanding of the copper related recombination and defect formation processes.

In order to be able to use recombination lifetime methods for the characterization of the quality of thin epitaxial silicon layers, it is necessary to understand the physical principles of the measurement in a layered structure. A correct interpretation of the measurement results requires a theoretical study of the generation, recombination and diffusion of the charge carriers in a two-layer structure. In this work, an analytical solution to the current continuity equation for excess carriers in an epitaxial structure under time dependent optical excitation was derived. In addition, some analytical approximations were developed and numerical calculations were made to check their accuracy. The built-in potential between the epitaxial layer and the substrate was taken into account and also the light induced barrier lowering was included in the model. It was found that under typical μ-PCD measurement conditions the barrier lowering is noticeable and can even change the effective lifetime by up to two orders

of magnitude. The same model was applied for internal gettering wafers to characterize the gettering sites in the bulk.

There is a lot of experimental data on iron gettering by oxide related defects in the literature. These experiments were often made at high supersaturation and resulted in diffusion limited precipitation, where each oxide precipitate was an active gettering sink. This work studied the internal gettering of iron at varying supersaturation levels. It was found that the gettering efficiency depends strongly on the initial iron concentration and considerably high supersaturation is needed to initiate the gettering. The results were explained by the nucleation kinetics: Iron nuclei, which are too small to be detected as such, are formed at low temperature. The nuclei can then have a crucial role in the next annealing step at a higher temperature, when iron diffusivity is increased and the growth of precipitates is facilitated. The gettering process can thus be considered as a diffusion limited process but not all oxide precipitates are necessary active gettering sites. It was concluded that iron precipitation at low supersaturation has similarities to oxygen precipitation. Although the experiments reported in this thesis imply that internal gettering of low levels of iron (less than 10^{12} cm^{-3}) is difficult under practical annealing conditions, an interesting question remains to be further examined: Is there any way to getter the low levels of iron by IG? Now with the increased understanding of the iron precipitation behavior, it might be possible to find an efficient Low-High anneal for the gettering of low levels of iron.

Iron dissolution was studied experimentally and an empirical formula was presented, which allows the simulation of an arbitrary thermal budget. The experimental results imply that there is a strong binding energy between the gettered iron and oxide precipitates at the given conditions. In the future, it would be interesting to study whether the dissolution process is diffusion limited, similar to gettering, when the driving force for dissolution is higher. That is, when the level of undersaturation is higher.

References

[1] G. E. Moore, Electronics 38, 114 (1965).

[2] P. Bai, C. Auth, S. Balakrishnan, M. Bost *et al*., Proc. IEEE International Electron Devices Meetings, 2005, p.570.

[3] A. A. Istratov, H. Hieslmair, and E. R. Weber, Appl. Phys. A 70, 489 (2000).

[4] H. Huff, J. Electrochem. Soc. 149, S35 (2002).

[5] G. Zoth, W. Bergholz, J. Appl. Phys. 67, 6764 (1990).

[6] L. Jastrzebski, O. Milic, M. Dexter, J. Lagowski, D. DeBurk, K. Nauka, R. Witowski, M. Gordon, E. Persson, J. Electrochem. Soc. 140, 1152 (1993).

[7] D.K. Schroder, IEEE Circuits and Devices 14, 14 (1998).

[8] D.K. Schroder, IEEE Transactions on Electron Devices 44, 160 (1997).

[9] D. K. Schroder, Mater. Sci. Eng. B91, 196 (2002).

[10] D.K. Schroder, Semiconductor Material and Device Characterization, 2nd Ed., New York: Wiley , 1998, ch 7.

[11] V. Lehmann, H. Föll, J. Electrochem. Soc. 135, 2831 (1988).

[12] G. Zoth and W. Bergholz, J. Appl. Phys. 67, 6764 (1990).

[13] M. Yli-Koski, M. Palokangas, V. Sokolov, J. Storgårds, H. Väinölä, and H. Holmberg, Physica Scripta, Vol. T101, 86 (2002).

[14] M. Yli-Koski, M. Palokangas, A. Haarahiltunen, H. Väinölä, J. Storgårds, H. Holmberg, and J. Sinkkonen, Journal of Physics: Condensed Matter 14, 13119 (2002).

[15] A. A. Istratov and E. R. Weber, J. Electrochem. Soc. 149, G21 (2002).

[16] A. A. Istratov, H. Hedemann, M. Seibt, O. F. Vyvenko, W. Schröter, T. Heiser, C. Flink, H. Hieslmair, and E. R. Weber, J. Electrochem. Soc. 145, 3889 (1998).

[17] R. Sachdeva, A.A. Istratov, and E. R. Weber, Appl. Phys. Lett. 79, 2937 (2001).

[18] A. Bazzali, G. Borionetti, R. Orizio, D. Gambaro, and R. Falster, Mat. Sci. Eng. B36, 85 (1996).

[19] Silvaco ATLAS Device Simulation Software, Version 5.0.0.R, Copyright 2004 Silvaco International.

[20] PC1D Simulation Software, Version 5.3, Copyright 1998 University of New South Wales, P. Basore and D. Clugston.

[21] M. B. Shabani, S. Okuuchi, and Y. Shimanuki, in Analytical and Diagnostic Techniques for Semiconductor Materials, Devices, and Processes, B.O. Kolbesen, C. Claeys, P. Stallhofer, F. Tardif, J. Benton, T. Shaffner, D. Schroder, S. Kishino, and P. Rai-Choudhury, Editors, PV 99-16, p. 510, The Electrochemical Society Proceedings Series, Pennington, NJ (1999).

[22] M. Boehringer, J. Hauber, S. Passefort, and K. Eason, J. Electrochem. Soc. 152, G1 (2005).

[23] D.A. Ramappa and W. B. Henley, Appl. Phys. Lett. 72, 2298 (1998).

[24] W. B. Henley and D.A. Ramappa, Appl. Phys. Lett. 74, 278 (1999).

[25] D.A. Ramappa, Appl. Phys. Lett. 76, 3756 (2000).

[26] A. Belayachi, T. Heiser, J. P. Schunck, and A. Kempf, Appl. Phys. A 80, 201 (2005).

[27] J. E. Park, D. K. Schroder, S. E. Tan, B. D. Choi, M. Fletcher, A. Buczkowski, F. Kirscht, J. Electrochem. Soc. 148, G411 (2001).

[28] D. K. Schroder, B. D. Choi, S. G. Kang, W. Ohashi, K. Kitahara, G. Opposits, T. Pavelka, J. Benton, IEEE Transactions on Elecron Devices 50, 906 (2003).

[29] H. Takahashi and T. Maekawa, Jpn. J. Appl. Phys. 39, 3854 (2000).

[30] T. Hara, F. Tamura, and T. Kitamura, J. Electrochem. Soc. 144, L54 (1997).

[31] T. Pavelka, Gate Dielectic Integrity: Material, Process, and Tool Qualification, ASTM STP 1382, Eds. D. C. Gupta and G. A. Brown, American Society for Testing and Materials, West Conshohocken, PA, 2000, p.145.

[32] Y. Ogita, Semicond. Sci. Technol. 7, A175 (1992).

[33] Y. Ogita, J. Appl. Phys. 79, 6954 (1996).

[34] H. Takahashi and T. Maekawa, Jpn. J. Appl. Phys. 41, 1214 (2002).

[35] H. Väinölä, Master's Thesis, Electron Physics Laboratory, Helsinki University of Tehnology, 2000.

[36] D. K. Schroder, B. D. Choi, S. G. Kang, W. Ohashi, K. Kitahara, G. Opposits, T. Pavelka, J. Benton, IEEE Transactions on Elecron Devices 50, 906 (2003).

[37] P. Renaud and A. Walker, Solid State Tecnology 43, 143 (2000).

[38] J. Storgårds, H. Väinölä, M. Yli-Koski, and J. Sinkkonen, Physica Scripta Vol. T101, 61 (2002).

[39] M. Porrini and P. Tessariol, Mater. Sci. Eng. B73, 244 (2000).

[40] J. M. Hwang and D. K. Schroder, J. Appl. Phys. 59, 2476 (1989).

[41] M. L. Polignano, M. Bramilla, F. Cazzaniga, G. Pavia, and F. Zanderigo, J. Electrochem. Soc. 145, 1632 (1998).

[42] A. A. Istratov, H. Hieslmair, and E. R. Weber, Appl. Phys. A 70, 489 (2000).

[43] S. M. Myers, M. Seibt, and W. Schröter, Appl. Phys. Rev. 88, 3795 (2000).

[44] H. Hieslmair, A. A. Istratov, and E. R. Weber, Semicond. Sci. Tehnol. 13, 1401 (1998).

[45] A. L. Smith, K. Wada, and L. C. Kimerling, J. Electrochem. Soc. 147, 1154 (2000).

[46]A. Haarahiltunen, H. Väinölä, M. Yli-Koski, E. Saarnilehto, and J. Sinkkonen, J. Electrochem. Soc. Proceedings, Vol. 05, p. 135 (2004).

[47] D. Gilles, E. R. Weber, and S. -K. Hahn, Phys. Rev. Lett. 64, 196 (1990).

[48] F. S. Ham, J. Phys. Chem. Solids 6, 335 (1958).

[49] A. Istratov, H. Väinölä, W. Huber and E. R. Weber, Semicond. Sci. Technol. 20, 568 (2005).

[50] H. Hieslmair, A. A. Istratov, S. A. McHugo, C. Flink, T. Heiser, and E. R. Weber, Appl. Phys. Lett. 72, 1460 (1998).

[51] K. F. Kelton, R. Falster, D. Gambaro, M. Olmo, M. Cornara, and P. F. Wei, J. Appl. Phys. 85, 8097 (1999).

[52] H. Takeno, T. Otogawa, and Y. Kitagawara, J. Electrochem. Soc. 144, 4340 (1997).

[53] D. Kashchiev, Nucleation: Basic Theory with applications (Butterworth-Heinemann, Oxford, 2000), p. 77.

[54] A. Haarahiltunen, H. Väinölä, O. Anttila, E. Saarnilehto, M. Yli-Koski, J. Storgårds, and J. Sinkkonen, Applied Physics Letters (in press).

[55] H. Hieslmair, A. A. Istratov, S. A. McHugo, C. Flink, and E. R. Weber, J. Electrochem. Soc. 145, 4259 (1998).

[56] H. Takahashi, H. Yamada-Kaneta, and M. Suezawa, Jpn. J. Appl. Phys. 37, 1689 (1998).

[57] S. McHugo and C. Flink, Appl. Phys. Lett. 77, 3598 (2000).

[58] A. Belayachi, T. Heiser, J. P. Schunck, S. Bourdais, P. Bloechl, A. Huber and A. Kempf, Mater. Sci. Eng. B 102, 218 (2003).

[59] P. Zhang, H. Väinölä, A. Istratov, and E. R. Weber, Physica B, Vols. 340-342 pp. 1051-1055 (2003).

[60] D.A. Ramappa and W.B. Henley, J. Electrochem. Soc. 144, 4353 (1997).

[61] S. McHugo, E. R. Weber, M. Mizuno, and F.G. Kirscht, Appl. Phys. Lett. 66, 2840 (1995).

[62] M. Aoki and A. Hara, J. Appl. Phys. 74, 1440 (1993).

ISBN 951-22-7872-3
ISBN 951-22-7873-1 (PDF)
ISSN 1795-2239
ISSN 1795-4584 (PDF)